J Neurophysiol 102: 714–723, 2009.
First published May 27, 2009; doi:10.1152/jn.91366.2008.

Transient Signals Trigger Synchronous Bursts in an Identified Population of Neurons

Gary Marsat, Rémi D. Proville, and Leonard Maler
Department of Cellular and Molecular Medicine, University of Ottawa, Ottawa, Ontario, Canada

Submitted 30 December 2008; accepted in final form 19 May 2009

Marsat G, Proville RD, Maler L. Transient signals trigger synchronous bursts in an identified population of neurons. *J Neurophysiol* 102: 714–723, 2009. First published May 27, 2009; doi:10.1152/jn.91366.2008. It is an important task in neuroscience to find general principles that relate neural codes to the structure of the signals they encode. The structure of sensory signals can be described in many ways, but one important categorization distinguishes continuous from transient signals. We used the communication signals of the weakly electric fish to reveal how transient signals (chirps) can be easily distinguished from the continuous signal they disrupt. These communication signals—low-frequency sinusoids interrupted by high-frequency transients—were presented to pyramidal cells of the electrosensory lateral line lobe (ELL) during in vivo recordings. We show that a specific population of electrosensory neurons encodes the occurrence of the transient signal by synchronously producing a burst of spikes, whereas bursting was neither common nor synchronous in response to the continuous signal. We also confirmed that burst can be triggered by low-frequency modulations typical of prey signals. However, these bursts are more common in a different segment of the ELL and during spatially localized stimulation. These localized stimuli will elicit synchronized bursting only in a restricted number of cells the receptive fields of which overlap the spatial extent of the stimulus. Therefore the number of cells simultaneously producing a burst and the ELL segment responding most strongly may carry the information required to disambiguate chirps from prey signals. Finally we show that the burst response to chirps is due to a biophysical mechanism previously characterized by in vitro studies of electrosensory neurons. We conclude that bursting and synchrony across cells are important mechanisms used by sensory neurons to carry the information about behaviorally relevant but transient signals.

INTRODUCTION

Communication signals, including aggressive and courtship messages, contain crucial information for the survival of individuals. Sensory systems must accurately encode these messages so that they can be recognized and used to guide behavior. Many communication signals are repetitive and continuous such as anuran and insect songs (Gerhardt and Huber 2002), but others are brief and transient. Good examples of brief signals are the stop consonants of human speech: short broadband transient—such as /d/, /b/, /p/—that are crucial for speech comprehension (Fitch et al. 1997). Continuous signals can be encoded and described by ongoing, long stretches of neural activity, but transient signals must be accurately encoded by short spike sequences. It is not clear how neural codes and signal type match up so as to rapidly distinguish transient from continuous signals. Sensory processing in the electric fish provides an excellent system to study this question because its communication signals are composed of both continuous and transient components. Furthermore these signals are relatively simple, well characterized, and easy to replicate.

Apteronotus leptorhynchus emits a constant wave-like electric field (i.e., electric organ discharge, EOD) with males having higher frequencies than females (Maler 2007). When two fish are in proximity the summation of their EODs produces a sinusoidal AM (SAM), or beat, the frequency (equal to the difference of their EOD frequencies) of which serves to signal the sex of the participants (Hagedorn and Heilingenberg 1985; Zakon and Dunlap 1999). When two males with similar EOD frequencies interact, this results in a spatially diffuse (global) low-frequency continuous signal. This global signal activates a feedback mechanism that cancels the receptors' input in a subset of first-order electrosensory pyramidal neurons; in contrast, spatially localized stimuli are not cancelled but encoded in the firing rates of the pyramidal cells (Bastian 1996; Bastian et al. 2004). The low-frequency SAMs present during agonistic male interactions also evoke the production of brief EOD frequency increases (small chirps) that serve as a warning that physical aggression could follow (Hupé and Lewis 2008). Males tend to trade chirps, but a chirp ($<$20 ms) can occur in an unpredictable manner within a wide temporal window (200 to $>$800 ms) (Hupé and Lewis 2008; Zupanc et al. 2006). Chirps result in transient changes in the EOD amplitude superimposed on the slower beats. The vast majority of electroreceptors in this species are named P-units because they discharge probabilistically after each EOD cycle. In this paper, we will use the term electroreceptors to refer to P-units. Electroreceptors encode small chirps by increasing both their firing rate and synchrony (Benda et al. 2005 2006). These electroreceptors project topographically to three maps located in the centromedial, centrolateral, and lateral segment (CMS, CLS, and LS, respectively) of the laminar electrosensory lateral line lobe (ELL) (Carr et al. 1982; Heiligenberg and Dye 1982), where they contact several types of pyramidal neurons (Bastian and Courtright 1991; Maler et al. 1979). Pyramidal cells have spatially localized receptive fields (RFs) due to the topography of electroreceptor input (Bastian et al. 2002), while feedback input to their apical dendrites allows spatially diffuse global input to also influence pyramidal cell activity (Bastian et al. 2004). Local input to the RF of a pyramidal cell mimics natural stimulation during prey capture, and global stimulation mimics the communication signals that occur during social interactions (Babineau et al. 2006; Kelly et al. 2008).

Pyramidal cells of the ELL possess a thoroughly characterized bursting mechanism which has been shown to underlie the detection of prey (Oswald et al. 2004; Turner et al. 2002). It is, however, unknown how communication signals (i.e., chirps)

Address for reprint requests and other correspondence: G. Marsat; 451 Smyth Rd., Ottawa, Ontario K1H-8M5, Canada (E-mail: gmarsat@gmail.com).

are encoded in the ELL and whether bursts also play a role in this context. We made in vivo recordings of pyramidal cells from different regions of the ELL to describe their response to these stimuli. We identify the cells responding to each type of signal and reveal how different subsets of bursting cells are activated by prey versus communication stimuli. Finally we examine the intrinsic and networks properties leading to bursts and burst regulation in response to chirps.

METHODS

Surgery and electrophysiology

Apteronotus leptorhynchus were put under general anesthesia by adding tricaine methanesulfonate (Finquel MS222, Argent Chemical Laboratories, Redmond, WA) to the water. The fish was respirated with this water to provide oxygen while keeping it under general anesthesia. A circular portion of skin on top of the skull was removed, and local anesthetic was applied to the wound. The skull was glued to a post for stability. A portion of skull was removed to expose the area of the brain overlaying the ELL. Once the surgery completed, the fish was awakened by respirating it with anesthetic-free water; it was then immobilized with an injection of curare (pancuronium bromide). After surgery the fish was transferred to the experimental tank ($40 \times 45 \times 20$ cm) containing water kept between 25 and 27°C and with conductivity around 200 μS. The fish was submerged except the top-most portion of the skull where the opening was located. In vivo recordings were performed using metal-filled extracellular electrodes or KAc-filled borosilicate intracellular electrodes. Pyramidal cells can easily be identified by the anatomy of the ELL and overylying cerebellum as well as by their response properties. Mediolateral position and depth of penetration (in the dorsal-ventral plane) was monitored and used to estimate electrode placement relative to the three segments of the ELL. Anatomical studies have thoroughly characterized the position of the different segments of the ELL (Maler et al. 1991), and these measurements were used to improve the accuracy of electrode placement. In particular, depending on the rostrocaudal position of the electrode, each ELL segment can be found at characteristic distances from the dorsal surface of the brain. For example, a recording from a cell body 400 μm from the surface can only be from a cell of the lateral segment. Furthermore, cells in each segment differ in their temporal tuning properties (Krahe et al. 2008), and we therefore calculated the coherence of their response to random amplitude modulations (Fig. 5*D* and see following text) to confirm electrode placement. All experiments and protocols were approved by the University of Ottawa Animal Care Committee.

Stimulation

The unperturbed EOD was recorded between the head and the tail of the fish. Each EOD cycle triggered a sine-wave generator (195 Universal waveform generator, Fluke, Everett, WA) to output one cycle of a sinusoidal signal of frequency matching that of the fish's EOD. This sinusoidal output was amplitude modulated with our stimulus envelopes. Stimuli were attenuated (PA4, Tucker-Davis Technologies, Alachua, FL), isolated (Model No. 2200; A-M Systems, Carlsborg, WA) and delivered through two stimulation electrodes placed on either side of the fish, parallel to its longitudinal axis; this arrangement partially mimics the stimulus geometry of electrocommunication signals (Kelly et al. 2008) and is referred to as global stimulation because electroreceptors over the entire body surface are stimulated. Local stimulation was delivered through a dipole located a few millimeters away from the skin and centered on the cell's receptive field; this arrangement mimics the stimulus geometry induced by prey or other small objects. The size of the dipole was adjusted for each segment because cells of the lateral segment have larger receptive field than cells of the centromedial segment (Shumway 1989). After locating the cell's receptive field by finding the position of a local stimulation dipole that best excites the cell, an additional dipole was used to measure the amplitude of the stimulus near the cell's receptive field. The stimulation local dipole was positioned between—and equidistance to—the local recording dipole and the skin. For both local and global geometries, stimulus intensity was adjusted to obtain a difference of the amplitudes of the EOD between the top and the bottom of a beat cycle corresponding to ~15% of the baseline EOD amplitude. Therefore for each cell, the local and global stimulus intensity was approximately equal within the cells receptive field, and the only difference was the additional activation of global feedback networks during global stimulation (Bastian et al. 2004; Chacron et al. 2003).

The stimulus envelope of chirp stimuli consisted of a sinusoidal beat of 5 Hz punctuated every second by a chirp. Chirp shape was calculated, as previously described (Benda et al. 2005), assuming a Gaussian frequency increase in the EOD during chirping with a width of 14 ms (at 10% height), occurring at different phases of the beat (0, 1/2 π, π, 3/2 π) and various frequency increases (60, 100, 122 Hz). Chirps used for the analysis of the responses occurred at the bottom or the top of the beat (for E- and I-cells, respectively) and were frequency increases of 60 Hz.

Stimulation by modulating the fish's EOD as described in the preceding text replicates the AM elicited by a real chirping fish. Confirming the behavioral efficacy of such stimuli, we frequently observed male fish chirping in response to our AM stimulus in the same way it would if another fish was introduced in the tank. Furthermore, this method was shown to elicit the same response from the electroreceptors as stimulating with a mimic of the actual EOD of another fish (Benda et al. 2005).

We also used broad band noise signals (random amplitude modulations, RAM). The envelopes of RAM stimuli were Gaussian white noise with frequencies between 0 and 100 Hz. The amplitude these stimuli was adjusted as described in the preceding text but the SD of the RAM envelope was used as reference rather than the maxima of the beat envelope. All stimuli envelopes were sampled at 10 KHz.

Chirp data analysis

EXTRACELLULAR. Each 20-s chirp stimulus was presented at least twice to each cell, totaling a minimum of 40 chirps. Spike train were digitized at a sampling rate of 20 kHz. The spike trains were expressed as series of zeros and ones (1's when a spike occurred during the sampling interval) and then down-sampled to 2 kHz. For display purposes, spike trains were expressed as firing rate by convolving each binary spike train with a Gaussian kernel with an SD of 20 ms. For analysis, the spike trains where expressed as sequences of interspike intervals (ISIs). ISIs were considered to be part of the response to chirps if the spikes that define them occur within 50 ms of the beginning of the chirp. This time window encompasses the chirps and the period following the chirps where stimulus amplitude is still above average. The response to chirps (see Fig. 1*A*) is usually followed by quiescence, and all spikes visibly belonging to the chirp response occurred within that time window. Bursts in response to chirps were defined as a sequence of at least two spikes occurring in the 50-ms time window following the beginning of the chirp; their ISIs were only rarely >10 ms as shown in Fig. 1*B*. To avoid making assumptions about ISI threshold of bursts during the beat response, we chose a value of 10 ms because it corresponds to the theoretical limit of burst ISIs imposed by the intrinsic properties of the neurons (Turner et al. 2002). Furthermore, choosing only the shorter ISIs prevents any bias toward less synchronized events (i.e., longer ISIs) and thus allows a fair comparison of beat and chirps in Fig. 1*C, inset.*

INTRACELLULAR. Spike trains were digitized at a sampling frequency of 20 kHz. To analyze spike shape, we first removed membrane fluctuation caused by synaptic potentials: we averaged the response of the cell to several presentations of the stimulus while the

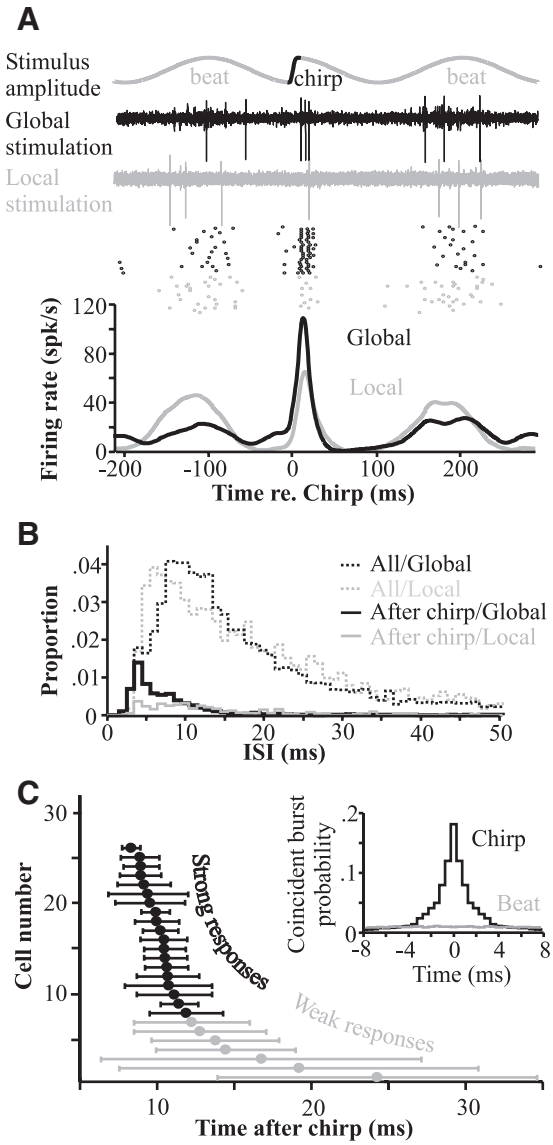

FIG. 1. Chirps trigger synchronized bursts. *A*: response of E-type pyramidal cells to chirp stimuli delivered locally or globally. The stimulus (*top*) is composed of a sinusoidal beat of 5 Hz (mimicking summation of the EODs of 2 male fish) punctuated by chirps. The strength of the stimulus results in a modulation of ~15% of the baseline electric organ discharge (EOD) amplitude. We show an example of a cell (raw traces and raster plots) responding to local and global stimuli and the mean firing rate of lateral segment (LS) E-cells ($n = 26$). Cells with high baseline firing rates (>23 Hz) were not included in the average, they are considered separately in Fig. 3. *B*: interspike interval (ISI) distribution of all evoked ISIs (chirps + beat) and of chirp-evoked ISIs. *C*: synchrony and reliability of the chirp-response. Each dot indicates the mean ± SD timing of the 1st spike of the response relative to the onset of the chirp. The hatched histogram shows the number of cells whose mean response falls in each 1-ms bin. Cells that responded with >1 spike in ≥50% of the cases are labeled as strong responses (black dots). Inset: a cross-correlogram of burst timing across repetitions; it quantifies the reliability of burst timing. Only data from cells with strong responses were used. Black trace, computed using the chirp-evoked bursts; gray trace, beat-evoked bursts. During the beat, bursts are defined as successive spikes with ISIs <10 ms.

cell was hyperpolarized (thus preventing spiking). We also averaged the spiking responses to the chirps after having removed the action potentials. To remove the spikes, we simply replaced each spike by a membrane potential that starts at the same value as the one found immediately preceding a spike and changing linearly to reach the value immediately following the spike. Spike beginning and end was selected based on the mean spike shape and encompassed the spike afterpotential. The average hyperpolarized response was scaled to have the same SD as the spiked-removed-spiking response. This ensured a good match between the size of the PSP during spiking and during hyperpolarization. The scaled hyperpolarized average was subtracted from each spiking response. We also tried using the average spike-removed-spiking response for the subtraction (no scaling) but found no qualitative difference in the results. We acknowledge that the small IPSPs that could participate in the evoked response might reverse in polarity during hyperpolarization, but this does not affect our conclusions because having the nonreversed IPSP polarity would increase the difference observed. Furthermore any potential bias would be similar for local and global stimulation and would therefore not affect their comparison (Fig. 7*C*).

The spikes were then classified depending on their timing relative to the stimulus in one of four categories: spontaneous spike (no stimulation present), top of the beat (occurring between phase 1/2 π and phase 5/4 π, where 0 and π are the bottom and top of the beat, respectively), the bottom of the beat (between phases 3/2 π and 1/4 π), or after a chirp (within 50 ms of its beginning). Beat cycles were divided this way to divide portions of the stimulus where excitation from electroreceptors dominate from those where excitation from feedback dominate in E-cells. Spikes were included in the average only if they were not followed by another spike within 20 ms to avoid distortion of the spike shape average by subsequent spikes. The size of the after-potentials were quantified by comparing the difference D between the shape of spontaneous spikes, $S_{sp}(t)$ and that of spike in other categories, $S_{st}(t)$ according to: $D = \sum_{t=0}^{w} S_{st}(t) - S_{sp}(t)$ where $t = 0$ is the time where the descending phase of the spike crosses baseline (baseline is defined by the average potential 5–10 ms before the spike) and $w = 20$ ms.

RAM stimuli analysis

One to 2 min of stimulation with RAM stimuli were used for analysis. We discarded the first second of stimulation during which firing rate might adapt. The burst threshold (measured from the spike trains autocorrelation) (Chacron and Bastian 2008) and the smallest ISI in the response of each cell were averaged across cells to obtain the range of burst ISI displayed in Fig. 5*C*.

Coherence was calculated by dividing the spike trains into three different variables: a burst-train containing only the first spike of each burst (bursts are thus considered unitary event the timing of which is that of its 1st spike), a single spike train containing none of the spike within bursts, and an original spike train containing all spikes. These spike trains were used to calculate the stimulus-to-response coherence as follows: $C(f) = |P_{sx}(f)|^2/|P_{ss}(f)P_{xx}(f)|$ where $P_{ss}(f)$ and $P_{xx}(f)$ are the power spectral density of the stimulus and the spike train, respectively, and $P_{sx}(f)$ their cross-spectral density. Coherence varies between 0 and 1 and quantifies how well the spike train reflects, in a linear manner, the modulation in the stimulus at each frequency. All data analysis was performed using Matlab (Mathworks, Natick, MA).

RESULTS

Synchronized bursts in response to chirps

Pyramidal cells of the ELL come in two main classes: E- and I-cell types (Maler 1979; Saunders and Bastian 1984). E-cells have basal dendrites that receive direct excitatory input from electroreceptors and respond to an increase in EOD amplitude. In contrast, I-cells receive electrosensory input via an interposed inhibitory interneuron and therefore respond to a decrease in EOD amplitude (they are inhibited by an EOD amplitude increase). A subset of E-cells of the LS of the ELL consistently produce a high-frequency burst in response to

globally presented chirps (Fig. 1*A*); in contrast, these cells respond only poorly to the low-frequency beat due to an active cancellation mechanism dependent on global feedback (Bastian 1996). A similar bursting response is observed for a variety of small chirps (Fig. 2). The chirp-evoked bursts therefore constitute the shortest ISIs of the entire response (Fig. 1*B*). During spontaneous activity, some cells fire spikes at precise time relative to the EOD cycle (phase-locking); however, spikes of chirp-evoked bursts were not phase-locked to the EOD (i.e., vector strength did not reach significance; Raleigh test, $P > 0.3$ for all cells), suggesting that the precise timing of these spikes was not directly determined by the synchronous firing of electroreceptors after each EOD cycle. The same stimulus delivered locally within the cell's RF does evoke a stronger response to the beat stimulus (Fig. 1*A*) because local stimulation does not activate the feedback cancellation mechanism (Bastian 1996). Local stimulation does not, however, elicit bursting in response to chirps [global burst ISI = 5.8 ± 5 (SE) ms; mean local discharge ISI = 15.8 ± 12.3 ms; paired *t*-test, $P < 0.02$]; this is the case even though the local stimulus has the same intensity (within the cell's receptive field) as the global stimulus, reinforcing the idea that direct electroreceptor input is insufficient to induce bursting and that network dynamics are also required. As a result, with local stimulation, the relatively weak firing during the chirp is inconspicuous because responses to chirps and beat are similar. We note that local chirps were presented as an experimental probe and would not occur naturally during interaction with conspecifics or in the presence of prey.

We show in Fig. 1*C* that global chirps lead to a synchronized burst response in LS E-cells. Most cells responded reliably to chirps with a burst in the majority of trials (19 of 26 cells, labeled "strong responses"). Other cells (7 of 26) produced a burst in <50% of the cases. We believe that for these cells, the stimulus was not strong enough to elicit reliable bursts due to the location and orientation of its RF relative to a stimulus geometry that will not effectively activate sufficient receptors. For example, receptors located on the fish's back will be oriented parallel to iso-potential lines of the stimulus and thus cannot respond to it. The cells with strong responses all produced bursts within a time window of ~3.5 ms. Furthermore, for each cell the timing of the bursts is very reliable from trial to trial: in 2/3 of the cases, burst timing varies by <2 ms (Fig. 1*C, inset*). In contrast, bursting (i.e., ISI < 10 ms) during the beat was not only rare (Fig. 1*B*) but also unreliable in their timing (Fig. 1*C, inset*, compare gray and black curve). Over the whole population (weak + strong responses), synchronized bursts (i.e., within 3.5 ms of each other) will occur in response to a chirp in 42% of cells but in only 6% of cells during the beat. Considering there are 300 superficial/intermediate E-cells in the LS (Maler 2009), we estimate that synchronous bursting will occur in ≤126 superficial LS E-cells in response to chirps but in only 18 cells in response to a beat cycle. Thus synchronous bursting across a large number of these cells can unambiguously signal the occurrence of a chirp and distinguish chirps and beats.

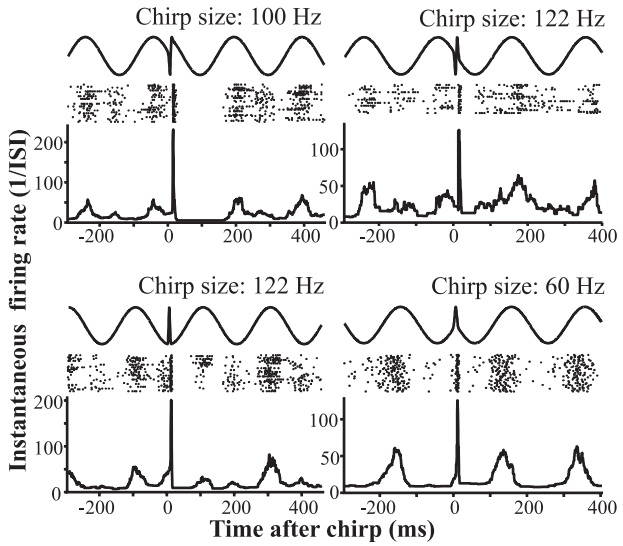

FIG. 2. Bursting response of 4 cells to chirps of different shapes. The shape of the chirp (shown at the top of each plot) is determined by the size of the frequency excursion of the EOD (60, 100, or 122 Hz), its length (which is held constant at 14 ms in these cases), and the phase of the beat at which it occurs. We display the responses to several repetitions of the stimulus as a raster plot and as a mean instantaneous firing rate. The instantaneous firing rate is quantified as the inverse of the ISI. This method allows us to conclude that, in each example, chirps are followed by ISIs in average <10 ms.

Chirp coding by an identified population of cells

Physiological and morphological features of ELL pyramidal cells covary: deep pyramidal cells (located in the ventral part of the pyramidal cell layer or within the granular layer of the ELL) have smaller apical dendrites and higher, more regular spontaneous firing rates than superficial ones (Bastian and Nguyenkim 2001). In Fig. 3, we examine the response of pyramidal cells as a function of their spontaneous firing rate. Figure 3*A* shows that E-cells with high firing rate (i.e., putative deep cell) fire strongly in response to both regular beat cycles and chirps and thus cannot specifically encode the occurrence of a chirp. The strongest selective burst response to chirps is observed in the superficial cells—those with lowest firing rates (Fig. 3*B*). This is presumably correlated with the extensive apical dendritic tree of these cells and emphasizes the importance of feedback networks in regulating even the fastest responses to transient and unexpected sensory input.

The I type pyramidal cells respond to decreases in EOD amplitude and were stimulated with an inverted chirp (Fig. 3*A*); it should be noted that both the upward stroke chirp (black trace) and its invert (gray trace) will be simultaneously present on opposite sides of the fish's body (Kelly et al. 2008). I-cells respond in a similar manner to beats and chirps and are therefore also not able to specifically signal the occurrence of a chirp (Fig. 3*B*).

Although all three ELL maps receive inputs from the same electroreceptors (Heilingenberg and Dye 1982), the LS is believed to be most important in processing transient communication signals (Metzner and Juranek 1997); we therefore next examined the response to chirps in the CMS and CLS. We show in Fig. 4 that neither E nor I pyramidal cells of the CMS and CLS respond strongly to chirps. Therefore we conclude that it is only the superficial E-cells of the LS that produce a strong spike burst in response to chirps.

Coding by bursts across topographic maps

Both in vivo and in vitro studies reveal differences in the temporal coding properties of E- and I-cells: in contrast to

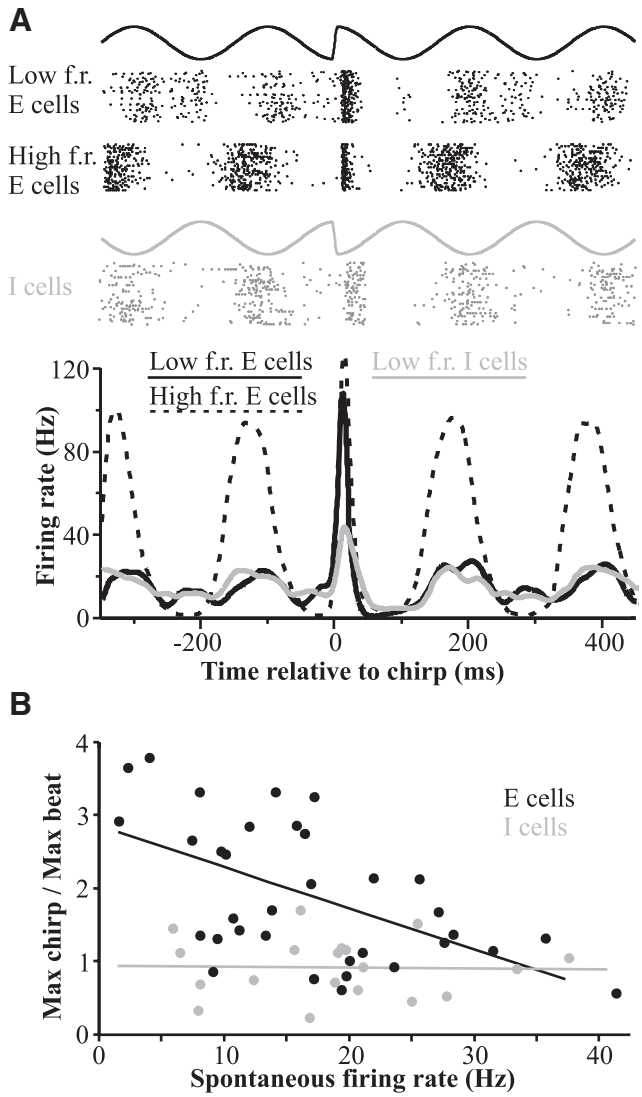

FIG. 3. Responses to chirps are salient only in a well defined subset of pyramidal cells. A. We show the responses of 3 types of cells (stimulus and raster plots for 3 cells at the top and mean response at the bottom): E-cells with low spontaneous firing rates (i.e., putative superficial and intermediate cells, $n = 26$), high-frequency E-cells (i.e., putative deep cells, $n = 8$) and low-frequency I-cells ($n = 14$). *B*: saliency of the chirp response as a function of cell type (E vs. I) and baseline firing rate. Baseline firing rate is a correlate of cell type (i.e., deep, intermediate, or superficial). For each chirp and beat cycle, the maximum response was defined as the inverse of the shortest ISI. These were used to calculate mean maximum response to beat and chirp and their ratio for each cell. Best-fit lines show the presence of a correlation for E-cells (slope ±95% confidence interval = 0.06 ± 0.03, $R^2 = 0.3$) and the lack thereof for I-cells (slope ±95% confidence interval = -10^{-3} ±0.02, $R^2 < 10^{-3}$).

E-cells, I-cells are low-pass across all segments (Krahe et al. 2008; Mehaffey et al. 2008). It is therefore not surprising that I-cells respond poorly to small chirps because these are high-frequency signals (Zupanc and Maler 1993). Temporal coding in E-cells varies across segments and the contribution of bursts for each segment is unknown. The lack of chirp-evoked bursts in CMS and CLS E-cells is certainly not due to the inability of these cells to burst. Indeed bursting in these pyramidal cells has been the focus of many studies both in vitro (e.g., Oswald et al. 2004; Turner et al. 2002) and in vivo (Gabbiani et al. 1996; Krahe et al. 2002). Replicating these studies, we stimulated the pyramidal cells with broad band noise signals (random AM, RAM; Fig. 5*A*). We show in Fig. 5*B* the ISI distribution of a representative cell from each segment. Bursting cells will have an initial peak in their autocorrelation function that we used to determine the burst threshold and the fraction of spikes that belonged to bursts (Chacron and Bastian 2008). Bursts were most frequent in CMS and CLS cells responding to local stimuli (Fig. 5*C*). The ISIs in these bursts were short and largely overlap the range of ISIs in the responses of LS E-cell to global chirps. Furthermore, these burst ISIs mostly fall below the theoretical limit of ~10 ms imposed by the bursting mechanism (Turner et al. 2002). However, cells of the LS and the CLS when stimulated globally produced relatively few bursts, and these bursts had longer ISIs. The ISIs of the bursts in LS in particular often exceeded the 10-ms limit for bursts based on a previously identified intrinsic mechanism (see following text).

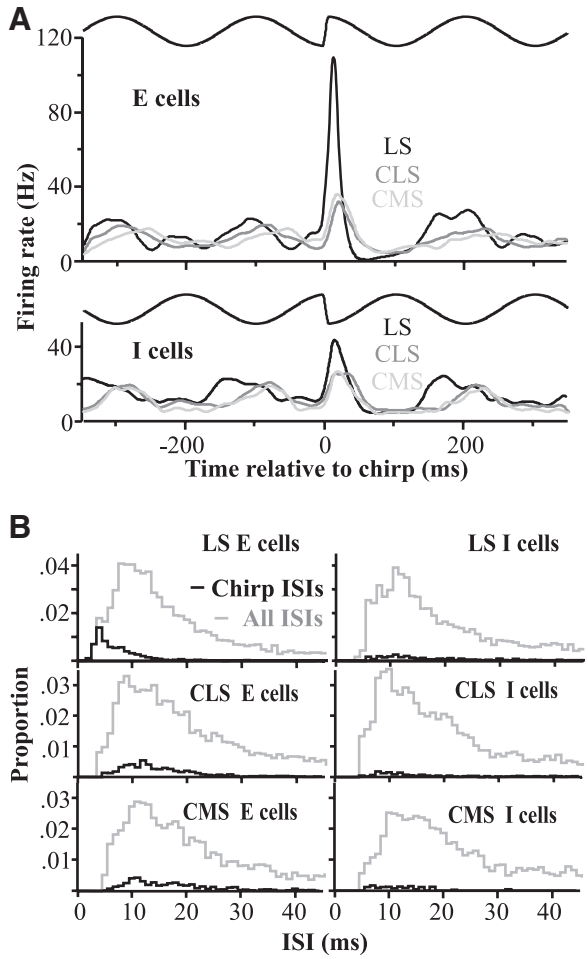

FIG. 4. Bursting in response to chirps is confined to the lateral segment of the ELL. *A*: responses of E- and I-cells from different segments. Each line represents the mean responses of E- and I-cells for the 3 ELL maps: centromedial (CMS; $n = 13$ E-cells and $n = 11$ I-cells), centrolateral (CLS; $n = 15$ E-cells and $n = 14$ I-cells), and LS ($n = 26$ E-cells and $n = 14$ I-cells). We only used the responses of superficial or intermediate cells E- and I-cells. The cells were categorized as superficial or intermediate if its spontaneous firing rate was <23 Hz. *B*: distribution of ISIs. In each plot, we show the distribution of all the ISIs in the response (beat and chirp, dashed gray line) and the distribution of ISI that follow chirps. ISIs following chirps are shorter in LS E-cells than in the other cell type (ANOVA followed by Tukey test, $P < 0.02$ for all comparisons with LS E-cells).

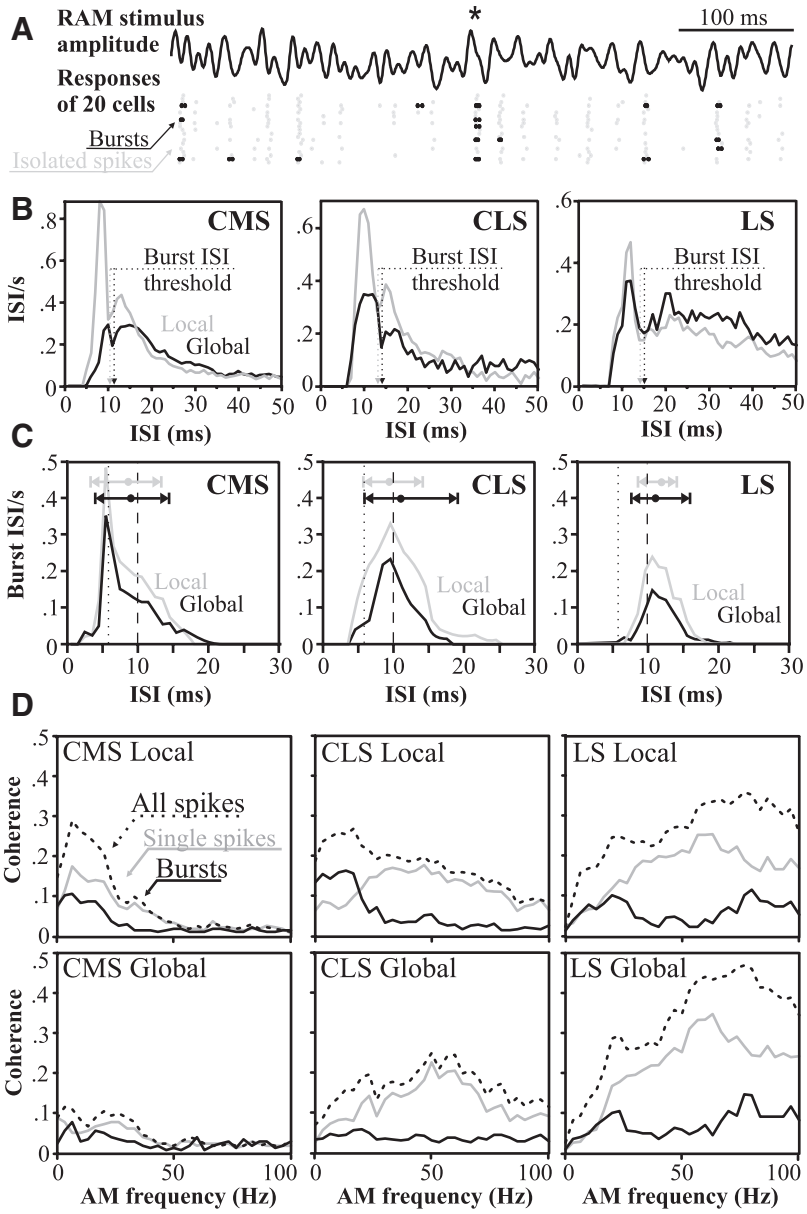

FIG. 5. Bursting and temporal coding across segments. *A*: example of responses to random amplitude modulation (RAM) stimuli. The peak in stimulus amplitude (*top trace)* marked with a star is the peak in this stimulus that triggers the most bursts. The raster plot of the responses of 20 different cells displays both isolated spikes (gray) and spikes within bursts (black). *B*: ISI distribution of 1 representative superficial E-cell from each segment when stimulated with local or global RAMs. For each distribution, the dashed line indicates the burst threshold (calculated from the autocorrelation; see *Experimental procedures*). Bin size: 1 ms. *C*: mean distributions of burst ISIs in responses of superficial/intermediate E-cells to RAM stimuli presented locally and globally. For each cell, we calculated the mean burst ISIs and their range. The average of these values across cells is shown with lines at the top of each graph where the circles shows the mean ISI of these bursts and the end-bars indicate their mean range (see *Experimental procedure*). The dotted line shows the mean ISI of chirp-evoked burst response in LS E-cells. The dashed line marks the theoretical maximal burst ISI imposed by the burst mechanism (Turner et al. 2002). Sample size: CMS = 13 cells, CLS = 15 cells, and LS = 26 cells. Bin size: 1 ms. *D*: mean coherence function of E-cells. The coherence between the whole spike train and the stimulus is shown (dashed) along with the coherence calculated using only bursts (black) or only single spikes (gray). Sample size: CMS = 13 cells, CLS = 15 cells, and LS = 26 cells.

We quantified the frequency tuning of the cells by calculating their stimulus-response coherence functions (Fig. 5*D*). The overall tuning of the cells match previously published results (Krahe et al. 2008). Specifically, high-frequency tuning is best in the LS, weaker in CLS cells (especially for local stimuli), and worst in CMS. Our analysis also confirms that bursts of the CMS and CLS were triggered by local low frequency—prey mimics AMs (Oswald et al. 2004). However, LS bursts were not only rare and composed of longer ISIs (Fig. 5*C*) but were also not specifically tuned to low frequencies (Fig. 5*D*). Nevertheless, global RAM stimuli could potentially trigger synchronous bursts in a proportion of LS E-cells. We selected the five amplitude peaks in the RAM stimulus that were most likely to trigger a burst in these cells (see example marked with a star in Fig. 5*A*). On average, these peaks triggered a burst in only 23% of the cells. This number provides an upper bound on the proportion of cells that will burst in response to this type of stimulus and corresponds to about half the cells that burst in response to chirps. These results indicate that bursts with very short ISIs (<10 ms) produced synchronously by a large proportion of LS E-cell clearly signal the occurrence of a chirp while for CMS/CLS E-cells bursts predominantly encode low-frequency local prey-like signals.

Burst mechanism and regulation

In vitro studies show that bursts in CMS cells are due to a well-described, ping-pong mechanism (Oswald et al. 2004; Turner et al. 1994, 2002): spikes back-propagate up the apical dendrites and cause a depolarizing afterpotential (DAP), thus increasing the probability of producing successive spikes with short ISIs (<10 ms). We hypothesized that the chirp-evoked bursts (short ISIs) of LS E-cells are also due to this mechanism. This hypothesis was investigated with in vivo intracellular recordings of LS pyramidal cells where, in addition to the spiking response, the stimulus-evoked synaptic response could be revealed by hyperpolarizing the cells. The neuron's resting membrane potential ranged from −55 to −70 mV, and similar

stimulus evoked responses were seen over this range. As expected from the extracellular recording, the global beat stimulus evoked only a weak modulation of the cell's membrane potential (Fig. 6*A*). The evoked compound EPSP rises faster and higher in response to chirps compared with beats (Fig. 6, *A* and *B*). However, it is important to note that while the local beat evoked membrane potential modulation increases (Fig. 6*C*), chirp-evoked EPSPs do not differ for local versus global stimulation (Fig. 6, *C* and *D*) and even with more intense local stimulation the cells did not burst (data not shown). The chirp-evoked EPSP initiated a first spike precisely at its steep onset for both local and global stimulation (Fig. 6*D*). As in slice recordings, spontaneous spikes of E-cells were followed by a large SK-mediated afterhyperpolarization (AHP) (Ellis et al. 2007). This is most obvious when comparing the shape of spike from an LS I-cell and E-cell (Fig. 7*A*) because, in agreement with the in vitro results, I-cells do not have this AHP. This comparison also highlights the fact that DAPs and AHPs are concurrent. With local stimulation the large AHP prevented the cell from immediately firing additional spikes and therefore bursting (Fig. 6, *top trace*). Under global stimulation the AHP appears to be reduced or truncated (*bottom trace*) permitting additional spikes to be fired within <10 ms.

To confirm this qualitative observation, we extracted the stimulus evoked AHP by subtracting the mean synaptic response of a cell from its spiking response. We used the average AHP of spontaneous spikes (i.e., no stimulation) as a reference

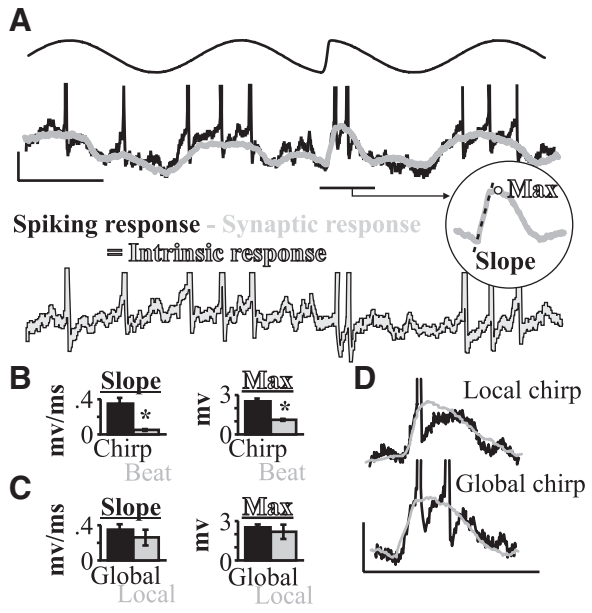

FIG. 6. Synaptic potential underlying chirp responses. *A*: the mean response of a cell while hyperpolarized (gray) represents the synaptic response to beat and chirp signals. When subtracted from the spiking response (black) we obtain the intrinsic spike-dependent response of the cell (*bottom*) to these signals; this potential is used in Fig. 7 for further analysis. *Inset*: the slope and maximum of the depolarization. *B*: mean ± SE ($n = 11$ cells) onset slope and maximum (relative to the mean membrane potential) of the depolarization caused by beat cycles and chirps while the cells are hyperpolarized. The stars indicate significant difference with the chirp-evoked response (paired *t*-test, $P < 0.05$). *C*: mean ± SE ($n = 11$ cells) onset slope and maximum (relative to the mean membrane potential) of the depolarization caused by chirps delivered locally or globally while the cells are hyperpolarized. Local and global response do not differ (paired *t*-test, $P > 0.1$). *D*: details of the mean depolarization cause by chirps in 1 cell while hyperpolarized (gray) along with an example of the spiking response (black). Scale bars: 2 mV, 100 ms.

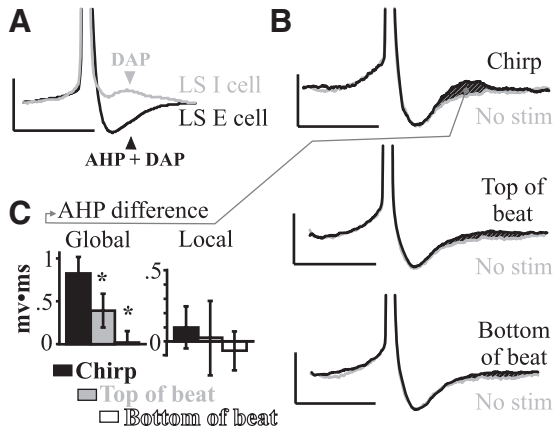

FIG. 7. Difference in spike-shape between chirp- and burst-triggered spikes. *A*: mean shape of the spontaneous spike of 1 I-cell (gray) and 1 E-cell (black) of the LS superimposed revealing the concurrence of the afterhyperpolarization (AHP) and the depolarizing afterpotential (DAP). In the LS, AHPs are present only in E-cells. *B*: mean spike shape of 1 cell during stimulation superimposed on the shape on spontaneous spikes (after subtraction of the synaptic response as in Fig. 6*A*, *bottom*). The hatched area highlights the difference between the 2 that we quantify in *C*. *C*: mean ± SE ($n = 11$ cells) differences in AHP size quantified as the difference between stimulus elicited spikes and spontaneous spikes. *, significant differences with chirp-induced spikes (ANOVA followed by Tukey test, $P < 0.05$). Scale bars: 5 mV, 10 ms.

to compare spikes occurring at different times relative to the stimulus (Fig. 7*B*). We found that spikes following a globally presented chirp have a shorter or smaller AHP and/or a larger DAP compared with spontaneous spikes whereas AHPs occurring at the top or the bottom of a beat cycle hardly differ from those of spontaneous spikes. We quantified this in Fig. 7*C* by subtracting the shape of spontaneous spikes to those in one of the other three categories (hatched area in Fig. 7*B*). The same analysis performed for responses to local stimuli show no difference in AHP shape compared with spontaneous spikes, indicating that global feedback input is necessary to regulate the spike afterpotential and thus bursting.

The AHP and DAP overlap in time and their relative magnitude regulates the propensity to burst (Ellis et al. 2007). The timing of the second chirp-evoked spike corresponds with the timing of the DAP (Fig. 8*A*) demonstrating that chirp-evoked bursts are due to the same DAP-based mechanism responsible for detection of low-frequency AMs in CMS/CLS. However, we cannot determine whether this chirp-specific response is due to an increase of DAP magnitude, a decrease of

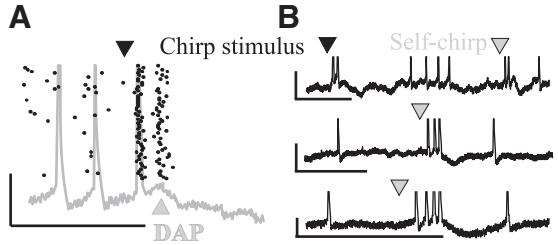

FIG. 8. DAP-based bursting in response to chirps. *A*: raster plot of many responses of a representative cell to the same chirp stimulus superimposed with its membrane potential during one of the responses were the DAP was clearly visible. The black arrow indicates the timing of the chirp. *B*: responses to artificial stimuli are similar to natural ones. We show responses of 3 cells to the fish's own chirps (gray arrow). In the 1st cell, the response to an artificial chirp (black arrow) is similar to the adjacent response to a self-chirp. Scale bars: 10 mV, 100 ms.

the AHP, or both. The specific expression of chirp-evoked DAP-mediated bursts is especially clear in the response to the fish's own chirps. Self-chirps are large signals and evoked strong bursts with the characteristics of the classic DAP-mediated burst: speeding up of spike frequency and a large AHP following the burst (Fig. 8*B*) (Turner et al. 2002).

DISCUSSION

Previous studies by Metzner and colleagues revealed the importance of the LS segment for electrosensory mediated communication. Lesioning the LS greatly impaired the chirp response (Metzner and Juranek 1997), whereas leasioning the CMS did not. Furthermore, pyramidal cells of this segment were also most sensitive to transient communication stimuli (Metzner and Heiligenberg 1991). Our study indicates that, in *Apteronotus*, a specific population of cells, superficial LS E-cells, most clearly signal the occurrence of small chirps presented in the context of same-sex interactions. Of all the stimuli tested, only chirps could trigger synchronous bursting in the majority of superficial and intermediate LS E-cells. These bursts are due to the same DAP-based mechanism that enables E-cells of CMS/CLS to respond to low-frequency local prey signals (Oswald et al. 2004). Bursts are rarely elicited by locally presented chirps that fully activate the electroreceptor input to LS E-cells and evoke compound EPSPs of the same magnitude as those evoked by globally presented chirps. Furthermore, only cells with extensive apical dendritic trees (superficial pyramidal cells) responded strongly to chirp stimuli. Therefore although chirps are brief unpredictable signals, network interactions likely including feedback, are also required to evoke bursts. The first chirp-evoked spike is due to a strong electroreceptor input evoked by the chirp (Benda et al. 2005, 2006), but it is a network regulation that permits the DAP to overcome the normally strong AHP of LS E-cells and thus generate bursts specifically in response to chirps.

Chirps are predominantly high-frequency signals; Zupanc and Maler (1993) estimated that they contained frequencies ranging from 50 to 100 Hz. Krahe et al. (2008) have recently shown that E-cells in the three ELL maps of electroreceptor input are tuned, in vivo, to different frequency ranges (also see Fig. 5). CMS E-cells are tuned to low frequencies, whereas those in LS are tuned to the highest frequencies and are high-pass to both local and global signals; CLS E-cells are intermediate in their frequency tuning and respond to high-frequency signals only when they are presented globally. Similar results have been reported for in vitro recordings (Mehaffey et al. 2008). A experimental and computational study (Middleton et al. 2009) has demonstrated that the frequency tuning difference across the ELL segments is due to the combination of the pyramidal cell intrinsic properties revealed by Mehaffey et al. (2008) and the relative size of the receptive fields in the ELL segments—large in LS, small in CMS, and intermediate in size in CLS (Maler 2009). The lack of response of CMS E-cells to chirps is therefore likely a simple consequence of their low-pass tuning because I-cells in all three ELL maps are low-pass (Krahe et al. 2008; Mehaffey et al. 2008), the same reasoning also suggests that they are unlikely to respond to chirps. CLS E-cells do encode high frequencies but less effectively than LS E-cells (Fig. 5*D*) (Krahe et al. 2008). This may account in part for their weak response to chirps but is unlikely to be the full explanation because their response to chirps is no better than that of CMS E-cells (Fig. 4) despite their stronger response to high-frequency signals (Fig. 5*D*) (Krahe et al. 2008). Simple tuning to high frequencies also cannot explain the lack of response of LS E-cells to locally presented chirps. In addition, the strong response of LS E-cells to globally presented high-frequency sinusoidal amplitude modulations (SAMs) (Krahe et al. 2008) consists of isolated spikes (data not shown); the strong response of these cells to the high-frequency content of RAMs is also almost entirely due to isolated spikes (Fig. 5*D*). These results are expected based on an earlier study (Oswald et al. 2004) that showed (in vitro and in vivo) that only isolated spikes encode high-frequency signals in CMS and CLS. Subsequent studies further demonstrated that this was due to the synaptic inputs evoked by the high-frequency signals interfering with the burst generating mechanism (Doiron et al. 2007; Oswald et al. 2007). Most importantly we showed that bursts elicited by stimuli other than chirps do not occur synchronously across many LS E-cells. Our results therefore show that LS E-cell synchronized bursts provide a unique encoding of chirps.

This strong bursting response, however, occurs only in the context of a global signal. A sharp increase in EOD amplitude similar to chirps that is not accompanied by an ongoing beat—such as a step increase in EOD amplitude—does not lead to bursting (data not shown). Therefore although the exact nature of the network effects are not yet known, we hypothesis that the ongoing low-frequency beat preceding a chirp modulates the intrinsic properties of LS E-cells so as to enhance the relative size of the DAP during the chirp with respect to the SK channel-mediated somatic AHP. Interestingly, previous work has already demonstrated that the feedback pathway (activated by global signals) that cancels global low-frequency signals (Bastian et al. 2004) can also regulate bursting (Bastian and Nugyenkim 2001; Chacron and Bastian 2008). Further studies will be required to determine whether this feedback pathway is also responsible for regulating the burst response of LS E-cells to chirps.

We have also confirmed earlier work (Krahe et al. 2008) that demonstrated that E-cells of the CMS and CLS respond to local low-frequency (prey) signals. We have further shown that this low-frequency response is mediated mainly by bursts consistent with Oswald et al. (2004)'s in vitro demonstration that DAP-evoked bursts in CMS/CLS are coherent with low-frequency input. Interestingly, these cells express lower (CLS) or no (CMS superficial pyramidal cells) SK2 channels and the resultant medium AHP (Ellis et al. 2007). Thus the prominent AHPs of LS E-cells (Ellis et al. 2007) appear to prevent these cells from producing bursts in response to prey. Our results indicate that the same biophysical mechanism—dendrite-mediated DAPs—can produce bursts in response to entirely different classes of stimuli. The key appears to be both differential expression of additional channels (e.g., SK2) in LS E-cells and a network-mediated mechanism that controls the relative magnitude of the SK mediated AHP in comparison to that of the DAP.

The seminal work of Gabbiani et al. (1996), demonstrated that ELL pyramidal cell bursts act as feature detectors, and this research was refined to demonstrate that in CMS/CLS, the feature is a strong prey signal (Oswald et al. 2004). It has recently been shown that in CLS, local stimulation evoked

correlated bursting over a small contiguous population of E-cells (Chacron and Bastian 2008) and that this correlated bursting is dependent on feedback input. Bursting in CMS/CLS is triggered by relatively large peaks in the stimulus compared with the portions of stimulus that elicit isolated spikes or no spiking (Laing et al. 2003). It therefore appears that synchronized bursting might also signal the presence of unexpectedly large prey signals with the spatial extent of synchronization corresponding to the localized signal. Note that feedback networks are also required for the prey-evoked burst response.

Remarkably it appears that our results might also generalize to other sensory systems and different burst mechanisms. In the visual system, unexpected reversal of motion direction causes a synchronized burst in a subpopulation of retinal ganglion cells (Schwartz et al. 2007); it has further been shown that this is a nonlinear network effect. In the cricket auditory system, synchronized bursting plays a role in the detection and localization of unexpectedly large predator signals (Marsat and Pollack 2006, 2007). This coding principle was also recently demonstrated in the basal forebrain of rats where strong bursting in a neural ensemble is triggered by motivationally salient and unexpected stimuli (Lin and Nicolelis 2008).

In the lateral geniculate nucleus, bursting has been associated with sudden changes in contrast as occur when an object moves into the cell's RF (Leisica and Stanley 2004). Here again the role of bursting is to signal salient signals, although they rely on a different burst-generating mechanism (Leisica et al. 2006). Our hypothesis implies that the LGN burst response will also be locally synchronized.

Our results, together with previous studies, show that in two different contexts, synchronous bursts of spikes encode the occurrence of unexpected and transient signals that are behaviorally relevant for the electric fish. We suggest that a similar coding scheme is in place in widely different systems and therefore hypothesize that synchronized bursting will be commonly observed in sensory systems as a means to signal behaviorally relevant but unpredictable transient signals. Unlike previous work, we propose a general principle relating sensory bursts to the nature of the signals they encode. The transient and unexpected nature of these sensory signals suits their encoding by synchronized bursts because both bursts and synchronized spikes are reliably transmitted across synapses and easily distinguished from background activity (Jermakowwicz and Casagrande 2007; Krahe and Gabbiani 2004; Lisman 1997). Furthermore, bursts and synchronous spiking, like the events they encode, can be short but are information rich signals (Chacron et al. 2004; Jermakowwicz and Casagrande 2007). The combination of these two powerful neural codes ensures that the occurrence of transient but important sensory events is readily detectable in downstream networks.

ACKNOWLEDGMENTS

We thank J. Benda, W. Ellis, A. Longtin, and J. Middleton for technical help or useful discussions.

GRANTS

This research was supported by Canadian Institute of Health Research grants to G. Marsat and L. Maler.

REFERENCES

Babineau D, Longtin A, Lewis JE. Modeling the electric field of weakly electric fish. *J Exp Biol* 209: 3636–3651, 2006.

Bastian J. Plasticity in an electrosensory system. I. General features of a dynamic sensory filter. *J Neurophysiol* 76: 2483–2496, 1996.

Bastian J, Chacron MJ, Maler L. Receptive field organization determines pyramidal cell stimulus-encoding capability and spatial stimulus selectivity. *J Neurosci* 22: 4577–4590, 2002.

Bastian J, Chacron MJ, Maler L. Plastic and non-plastic pyramidal cells perform unique roles in a network capable of adaptive redundancy reduction. *Neuron* 41: 767–779, 2004.

Bastian J, Courtright J. Morphological correlates of pyramidal cell adaptation rate in the electrosensory lateral line lobe of weakly electric fish. *J Comp Physiol [A]* 168: 393–407.

Bastian J, Nguyenkim J. Dendritic modulation of burst-like firing in sensory neurons. *J Neurophysiol* 85: 10–22, 2001.

Benda J, Longtin A, Maler L. Spike-frequency adaptation separates transient communication signals from background oscillations. *J Neurosci* 25: 2312–2321, 2005.

Benda J, Longtin A, Maler L. A synchronization-desynchronization code for natural communication signals. *Neuron* 52: 347–358, 2006.

Carr CE, Maler L, Sas E. Peripheral organization and central projections of the electrosensory nerves in gymnotiform fish. *J Comp Neurol* 211: 139–153, 1982.

Chacron MJ, Bastian J. Population coding by electrosensory neurons. *J Neurophysiol* 99: 1825–1835, 2008.

Chacron MJ, Doiron B, Maler L, Longtin A, Bastian J. Non-classical receptive field mediates switch in a sensory neuron's frequency tuning. *Nature* 423: 77–81, 2003.

Chacron MJ, Longtin A, Maler L. To burst or not to burst? *J Comput Neurosci* 17: 127–136, 2004.

Doiron B, Oswald AM, Maler L. Interval coding. II. Dendrite-dependent mechanisms. *J Neurophysiol* 97: 2744–2757, 2007.

Ellis LD, Mehaffey WH, Harvey-Girard E, Turner RW, Maler L, Dunn RJ. SK channels provide a novel mechanism for the control of frequency tuning in electrosensory neurons. *J Neurosci* 27: 9491–9502, 2007.

Fitch RH, Miller S, Tallal P. Neurobiology of speech perception. *Annu Rev Neurosci* 20: 331–353, 1997.

Gabbiani F, Metzner W, Wessel R, Koch C. From stimulus encoding to feature extraction in weakly electric fish. *Nature* 384: 564–567, 1996.

Gerhardt HC, Huber F. *Acoustic Communication in Insects and Anurans: Common Problems and Diverse Solutions.* Chicago, IL: University of Chicago Press, 2002.

Hagedorn M, Heiligenberg W. Court and spark: electric signals in the courtship and mating of gymnotid fish. *Anim Behav* 33: 254–265, 1985.

Heiligenberg W, Dye J. Labelling of electroreceptive afferents in a gymnotoid fish by intracellular injection of HRP: the mystery of multiple maps. *J Comp Physiol [A]* 148: 287–296, 1982.

Hupé GJ, Lewis JE. Electrocommunication signals in free swimming brown ghost knifefish, *Apteronotus leptorhynchus. J Exp Biol* 211: 1657–1667, 2008.

Jermakowicz WJ, Casagrande VA. Neural networks a century after Cajal. *Brain Res Rev* 55: 264–284, 2007.

Kelly M, Babineau D, Longtin A, Lewis JE. Electric field interactions in pair of electric fish: modeling and mimicking naturalistic inputs. *Biol Cybern* 98: 479–490, 2008.

Krahe R, Bastian J, Chacron MJ. Temporal processing across multiple topographic maps in the electrosensory system. *J Neurophysiol* 100: 852–867, 2008.

Krahe R, Gabbiani F. Burst firing in sensory systems. *Nat Rev Neurosci* 5: 13–23, 2004.

Krahe R, Kreiman G, Gabbiani F, Koch C, Metzner W. Stimulus encoding and feature extraction by multiple sensory neurons. *J Neurosci* 22: 2374–2382, 2002.

Laing CR, Doiron B, Longtin A, Noonan L, Turner RW, Maler L. Type I burst excitability. *J Comput Neurosci* 14: 329–342, 2003.

Lesica NA, Stanley GB. Encoding of natural scene movies by tonic and burst spikes in the lateral geniculate nucleus. *J Neurosci* 24: 10731–10740, 2004.

Lesica NA, Weng C, Jin J, Yeh CI, Alonso JM, Stanley GB. Dynamic encoding of natural luminance sequences by LGN bursts. *PLoS Biol* 4: e209, 2006.

Lin SC, Nicolelis MA. Neuronal ensemble bursting in the basal forebrain encodes salience irrespective of valence. *Neuron* 59: 138–149, 2008.

Lisman JE. Bursts as a unit of neural information: making unreliable synapses reliable. *Trends Neurosci* 20: 38–43, 1997.

Maler L. The posterior lateral line lobe of certain gymnotoid fish: quantitative light microscopy. *J Comp Neurol* 183: 323–363, 1979.

Maler L. Neural strategies for optimal processing of sensory signals. *Prog Brain Res* 165: 135–154, 2007.

Maler L. Receptive field organization across multiple electrosensory maps. I. Columnar organization and estimation of receptive field size. *J Comp Neurol* In press.

Maler L, Sas E, Johnston S, Ellis W. An atlas of the brain of the electric fish *Apteronotus leptorhynchus. J Chem Neuroanat* 4: 1–38, 1991.

Marsat G, Pollack GS. A behavioral role for feature detection by sensory bursts. *J Neurosci* 26: 10542–10547, 2006.

Marsat G, Pollack GS. Efficient inhibition of bursts by bursts in the auditory system of crickets. *J Comp Physiol [A]* 193: 625–633, 2007.

McCormick DA, Huguenard JR. A model of the electrophysiological properties of thalamocortical relay neurons. *J Neurophysiol* 68: 1384–1400, 1992.

Mehaffey WH, Maler L, Turner RW. Intrinsic frequency tuning in ELL pyramidal cells varies across electrosensory maps. *J Neurophysiol* 99: 2641–2655, 2008.

Metzner W, Heiligenberg W. The coding of signals in the gymnotiform fish *Eigenmannia*: from receptors to neurons in the torus semicircularis of the midbrain. *J Comp Physiol [A]* 169: 135–150, 1991.

Metzner W, Juranek J. A sensory brain map for each behavior? *Proc Natl Acad Sci USA* 94: 14798–14803, 1997.

Middleton JW, Longtin A, Benda J, Maler L. Postsynaptic receptive field size and spike threshold determine encoding of high frequency information via sensitivity to synchronous presynaptic activity. *J Neurophysiol* 101: 1160–1170, 2009.

Oswald AM, Chacron MJ, Doiron B, Bastian J, Maler L. Parallel processing of sensory input by bursts and isolated spikes. *J Neurosci* 24: 4351–4362, 2004.

Oswald AM, Doiron B, Maler L. Interval coding. I. Burst interspike intervals as indicators of stimulus intensity. *J Neurophysiol* 97: 2731–2743, 2007.

Saunders J, Bastian J. The physiology and morphology of two types of electrosensory neurons in the weakly electric fish *Apteronotus leptorhynchus. J Comp Physiol [A]* 154: 199–209, 1984.

Schwartz G, Taylor S, Fisher C, Harris R, Berry MJ, 2nd. Synchronized firing among retinal ganglion cells signals motion reversal. *Neuron* 55: 958–969, 2007.

Shumway CA. Multiple electrosensory maps in the medulla of weakly electric gymnotiform fish. I. Physiological differences. *J Neurosci* 9: 4388–4399, 1989.

Turner RW, Lemon N, Doiron B, Rashid AJ, Morales E, Longtin A, Maler L, Dunn RJ. Oscillatory burst discharge generated through conditional backpropagation of dendritic spikes. *J Physiol* 96: 517–530, 2002.

Turner RW, Maler L, Deerinck T, Levinson SR, Ellisman MH. TTX-sensitive dendritic sodium channels underlie oscillatory discharge in a vertebrate sensory neuron. *J Neurosci* 14: 6453–6471, 1994.

Zakon HH, Dunlap KD. Sex steroids and communication signals in electric fish: a tale of two species. *Brain Behav Evol* 54: 61–69, 1999.

Zupanc GK, Maler L. Evoked chirping in the weakly electric fish *Apteronotus leptorhynchus*: a quantitative biophysical analysis. *Can J Zool* 71: 2301–2310, 1993.

Zupanc GKH, Sîrbulescu RF, Nichols A, Ilies I. Electrical interactions through chirping behavior in the weakly electric fish, *Apteronotus leptorhynchus. J Comp Physiol [A]* 192: 159–173, 2006.